Contribution from the Department of Chemistry,
Georgetown University, Washington, D.C. 20057

Bonding in Crystals Containing One-Dimensional Bridged and Unbridged Group 11 and 12 Linear, Zigzag, and Helical Chains

C. X. Cui[†] and Miklos Kertesz*[,‡]

Received August 7, 1989

Metal-metal (Cu-Cu, Ag-Ag, Au-Au, Cd-Cd, and Hg-Hg) distances in d^{10} metal chains (formally d^{10}) exhibit a large variety, the closest contacts being even shorter than in the elemental metals. Extended Hückel calculations (EHT) have been performed on a number of crystals containing one-dimensional chains of group 11 and 12 transition-metal atoms and related silver-rich compounds. We find that from the point of view of metal-metal bonding, the compounds fall into two main categories. In the first group, in which an anion of a main-group atom is the bridging ligand, there is slight or no M-M bonding due to the effect of the ligand, which reduces the metal-metal bonding between naked d^{10} centers. The short M-M bond distances for some of these chains come from metal-metal coupling through ligands. A typical example of such a compound is Na_2CuP. In the second group of compounds in which bridging ligands are absent, such as $[Ag(CCR)_2(PPh_3)]_x$, there is some M-M bonding producing the short M-M bond distances. The analysis of orbital interactions shows that if the bridging ligand is a typical two-electron σ donor, such as CH_3^-, some metal-metal bonding is induced by the ligand. An EHT calculation on Ag_2O indicates that the color and conductivity for a number of silver-rich compounds result from excitation from oxygen 2p and metal 4d orbitals to metal 5s and 5p orbitals. MNDO calculations show that the helical conformation of mercuric sulfide and oxide can be attributed to the flatness of the torsional potential curves over a broad range of twist angles.

Direct and Indirect M-M Bonding in Chains of Cu, Ag, Au, Cd, and Hg

Numerous crystals containing chains of group 11 and 12 transition-metal atoms (Cu, Ag, Au, Cd, and Hg) have been synthesized and characterized in the past couple of decades,[1] as listed in Table I. The common feature of their structures is the existence of zigzag chains with an alternating arrangement of metal and main-group group 5 or 6 anions and a 2-fold screw axis of symmetry, where metal atoms form linear chains and are linearly coordinated by main-group anions and have a formal electronic configuration of d^{10}. Remarkably, the metal-metal separations are comparable to or shorter than those of the corresponding elemental metals in many of these crystals. The bond distances in metals Cu, Ag, Au, Cd, and Hg are 2.58, 2.88, 2.88, 2.97, and 2.99 Å, respectively.[2] Structures **1a-d** show some typical

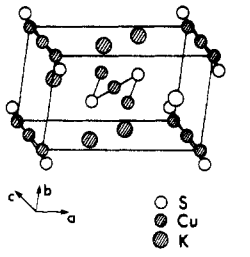

1a (KCuS)

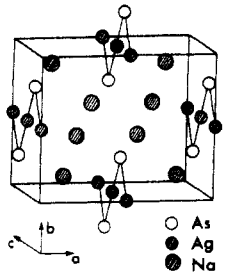

1b (Na_2AgAs)

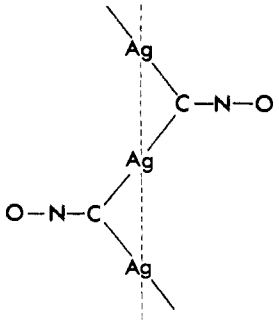

1c

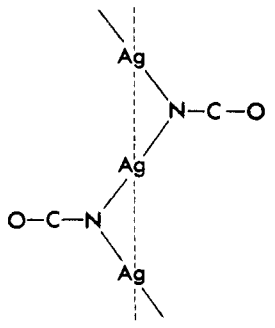

1d

chains. The crystals listed in Table I also show the following two features: (a) the separations of metal atoms range from the typical value of metal-metal bonding such as 2.56 Å in Na_2CuP to that for completely nonbonding region such as 3.30 Å in AuCl; (b)

Table I. A_nMR (n = 0, 1, 2) Type of Crystals Containing Bridged Linear Chains of d^{10} Cations

crystal	M	M-M, Å	R	q[a]	M-R, Å	MRM angle, deg	ref
Na_2CuP	Cu	2.65	P	-3	2.24	72.2	1a
KCuS (**1a**)		2.66	S	-2	2.13	76.6	1b
Na_2CuAs		2.67	As	-3	2.34	69.7	1c
K_2CuAs		2.96	As	-3	2.34	78.1	1c
Na_2CuSb		3.12	Sb	-3	2.50	76.9	1c
Na_2AgSb	Ag	2.89	Sb	-3	2.69	64.9	1d
Na_2AgAs (**1b**)		2.80	As	-3	2.52	67.5	1b
AgCNO (**1c**)		2.93	CNO[b]	-1	2.23	82.1	1e
K_2AgAs		3.01	As	-3	2.54	72.7	1a
K_2AgSb		3.14	Sb	-3	2.69	71.4	1a
K_2AgBi		3.17	Bi	-3	2.76	70.0	1a
AgNCO (**1d**)		3.19	NCO[c]	-1	2.12	98.0	1e
AuCl	Au	3.37	Cl	-1	2.36	92.0	1f
I-AuBr		3.47	Br	-1	2.40	92.3	1g
P-AuBr		3.04	Br	-1	2.44	77.1	1g
AuI		3.08	I	-1	2.62	72.0	1h
KAuS		3.26	S	-2	2.31	89.8	1i
KAuSe		3.34	Se	-2	2.41	87.7	1i
Na_2AuAs		2.88	As	-3	2.50	70.3	1j
Na_2AuSb		2.92	Sb	-3	2.64	66.9	1j
K_2AuSb			Sb	-3			1j
HgO	Hg	3.30	O	-2	2.05	109.0	1k
$HgNH_2Cl$		3.35	NH_2	-1	2.05	109.5	1l
$HgNH_2Br$		3.38	NH_2	-1	2.07	109.5	1m
K_2CdPb	Cd	3.23	Pb	-4	2.85	69.1	1n
K_2CdSn			Sn	-4			1n

[a] Formal charge on ligand. [b] Directly coordinating atom is C. [c] Directly coordinating atom is N.

[†] Permanent address: Institute of Theoretical Chemistry, Jilin University, Changchun, PRC.
[‡] Camille and Henry Dreyfus Teacher-Scholar, 1984-1989.

(1) (a) Savelsberg, G.; Schafer, H. *Z. Naturforsch.* **1977**, *B32*, 745. (b) Savelsberg, G.; Schafer, H. *Z. Naturforsch.* **1978**, *B33*, 711. (c) Eisenmann, B.; Savelsberg, G.; Schafer, H. *Z. Naturforsch.* **1976**, *B31*, 1344. (d) Schuster, H. U.; Newis, A.; Jung, W. *Z. Naturforsch.* **1979**, *B34*, 354. (e) Britton, D.; Bunitz, J. D. *Acta Crystallogr.* **1965**, *18*, 424; **1966**, *19*, 662. (f) Janssen, E. M. W.; Folmer, J. C. W.; Wiegers, G. A. *J. Less-Common Met.* **1974**, *38*, 71. (g) Janssen, E. M. W.; Wiegers, G. A. *J. Less-Common Met.* **1978**, *57*, P47. (h) Jagodzinski, H. *Z. Kristallogr., Kristallgeom., Kristallphys., Krystallchem.* **1959**, *112*, 80. (i) Klepp, O. K.; Bronger, W. *J. Less-Common Met.* **1978**, *75*, 128. (j) Mues, C.; Schuster, H. U. *Z. Naturforsch.* **1980**, *B35*, 1055. (k) Aurivillus, K. *Acta Chem. Scand.* **1950**, *4*, 1413; **1956**, *10*, 852. (l) Lipscomb, W. N. *Acta Crystallogr.* **1951**, *4*, 266. (m) Nijssen, L.; Lipscomb, W. N. *Acta Crystallogr.* **1952**, *5*, 604. (n) Matthes, R.; Schuster, H. U. *Z. Naturforsch.* **1979**, *B34*, 541.
(2) Wells, F. *Structural Inorganic Chemistry*; Clarendon: Oxford, England, 1984.

0020-1669/90/1329-2568$02.50/0

Table II. Crystals Containing Zigzag Chains of Cu, Ag, Au, and Hg

crystal	M	M-M, Å	MMM angle, deg	ref
CaCu	Cu	2.50	116.9	4a
SrAg	Ag	2.92	110.4	4a
BaAg (**3**)		3.09	107.4	4a
CaAg		2.88	107.8	4b
CaAu	Au			4b
Hg_3NbF_6	Hg	2.62	177.0	4c
		2.59	124.2	
		2.98		
$Ag_3(NSO_2)_3$ (**2**)	Ag	3.03	124.6	4d
Na_3AgO_2	Ag	3.04		4e
$Au[S(CH_2)_4]I$	Au	2.97	150.0	4f

the metal-ligand-metal (M-L-M) bond angles vary from 70 to 110°. Even when the same chain, $(CuAs^{2-})_x$, has different cations in the crystals, the separations of metal atoms can increase or decrease by 0.3 Å. These structural characteristics imply that the framework of such one-dimensional chains is not rigid. According to the previous analyses of the nature of metal-metal bonding in organometallic compounds of group 11 transition metals, the interaction between d^{10} centers are weakly attractive due to the mixing of metal s and p orbitals into d orbitals.[3] In this paper, the effect of ligands on the interactions between metal centers in these chains are investigated and found to be significant.

Some crystals[4] that are closely related to the chainlike structures listed in Table I are presented in Table II. From the point of view of ligand-metal coordination, the silver cations in $Ag_3(NSO_2)_3$ (**2**) are bound together directly, without the obvious as-

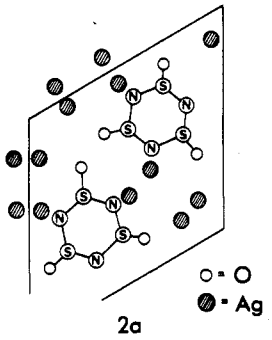

2a

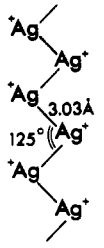

2b

sistance of bridging ligands. **2a** is one layer of a three-dimensional structure in the *ab* plane, and **2b** represents a silver cation chain in the *c* direction in this compound. In **2a**, there is one oxygen atom below each sulfur atom that can not be seen.

The electron count is different in the CaCu, SrAg, CaAg, and CaAu intermetallic phases, which crystallize in structures derived from the CrB structure.[2] They contain zigzag transition atom chains with bond distances similar to those of the corresponding transition-metal elements. The structure of a zigzag silver chain in the CaAg phase is shown in **3**. Similarities and

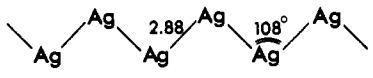

3

differences in bonding between the group 11 transition-metal atom chains in the crystals listed in Tables I and II will be discussed in this paper.

Polymers formed by mercury and main-group group 6 atoms have another important feature,[5] namely a 3-fold screw axis of symmetry. Their geometrical parameters are presented in Table III. There is a large group of chainlike compounds with bidentate bridging groups and corresponding large M-M separations such as AuCN and AgSCN.[6] For geometrical reasons, these do not exhibit any M-M bonding and are therefore omitted from our calculations.

Table III. HgR Helical Polymers

crystal	M-M, Å	M-R, Å	θ,[a] deg	bond angle, deg	ref
HgS (**4**)	3.10	2.36	120	105.0	5a
HgSe			120		5b
HgTe			120		5b
HgO (**4**)	3.28	2.05	120	108.0	5c

[a] Helical angle, θ, indicated in **5**.

The structures for HgS and HgO (**4**) are unique among those of monosulfides and monoxides. The screw modifications of

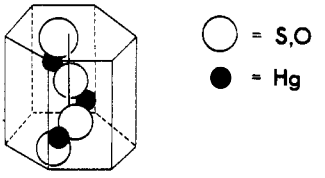

4

mercuric selenide and telluride only exist under high pressures.[5b] Polymeric mercuric sulfide is notable for its extraordinarily large optical rotatory power.[2] Many saturated σ-polymers have a helical configuration.[7] Basic geometrical parameters describing the helical polymer are illustrated in **5**, where ρ is the helical radius,

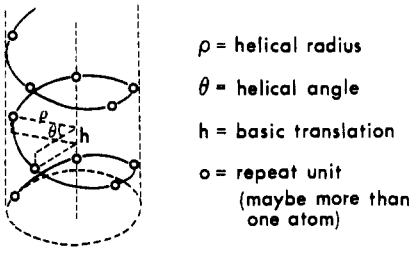

5

h is the translational part of the screw operation, and θ is the helical angle. What is the driving force toward a screw configuration in mercuric sulfide and oxide?

In this paper the questions we mentioned above, together with structural problems of related silver-rich compounds,[8] will be investigated by means of the crystal orbital approach based on extended Hückel theory (EHT)[9,10] as well as the MNDO (modified neglect of diatomic overlap)[11,12] crystal orbital approach.[13]

(3) (a) Merz, K. M., Jr.; Hoffmann, R. *Inorg. Chem.* **1988**, *27*, 2120. (b) Mehrotra, P. K.; Hoffmann, R. *Inorg. Chem.* **1977**, *17*, 2187. (c) Baetzold, R. C. *J. Chem. Phys.* **1971**, *55*, 4363. (d) Baetzold, R. C.; Mack, R. E. *J. Chem. Phys.* **1975**, *62*, 1513. (e) Yoshida, T.; Yamagata, T.; Tulip, T. H.; Ibers, J. A.; Otsuka, S. *J. Am. Chem. Soc.* **1978**, *100*, 2063. (f) Dedieu, A.; Hoffmann, R. *J. Am. Chem. Soc.* **1978**, *100*, 2074. (g) Avdeef, A.; Fackler, J. P., Jr. *Inorg. Chem.* **1978**, *17*, 2182. (h) Hollander, F. J.; Coucouvanis, D. *J. Am. Chem. Soc.* **1974**, *96*, 5646. (i) Mingos, D. M. P. *J. Chem. Soc., Dalton Trans.* **1976**, 1163. (j) Jiang, Y.; Alvarez, S.; Hoffmann, R. *Inorg. Chem.* **1985**, *24*, 749. (k) Cui, C. X.; Li, X. T.; Jiang, Y. *Acta Chim. Sinica* **1987**, *45*, 840.

(4) (a) Merlo, F.; Foranasini, M. L. *Acta Crystallogr.* **1980**, *37*, 500. (b) Merlo, F. *J. Less-Common Met.* **1982**, *86*, 241. (c) Brown, I. D.; Cutforth, B. D.; Davies, C.; Gillespie, R. J.; Irehrod, P. R.; Vekris, J. E. *Can. J. Chem.* **1974**, *51*, 971. (d) Dulgaard, G. A. P.; Hazell, A. C.; Hazell, R. G. *Acta Crystallogr.* **1974**, *B30*, 2721. (e) Schenk, F.; Hoppe, R. *Naturwissenschaften* **1969**, 414. (f) Ahrland, S.; Noren, B.; Oskarsson, A. *Inorg. Chem.* **1985**, *24*, 1330.

(5) (a) Aurivillus, K. *Acta Chem. Scand.* **1965**, *19*, 522. (b) Mariano, A. N.; Warekois, E. P. *Science* **1963**, *142*, 672. (c) Aurivillus, K. *Acta Chem. Scand.* **1958**, *12*, 1297.

(6) Adams, D. M. *Inorganic Solids*; John Wiley & Sons: New York, 1974.

(7) Cui, C. X.; Kertesz, M. *J. Am. Chem. Soc.* **1989**, *111*, 4216.

(8) For a review, see: Jansen, M. *Angew. Chem., Int. Ed. Engl.* **1987**, *26*, 1098.

(9) Hoffmann, R. *J. Chem. Phys.* **1963**, *91*, 2690.

(10) Whangbo, M. H.; Hoffmann, R. *J. Am. Chem. Soc.* **1978**, *100*, 6093.

(11) (a) Dewar, M. J. S.; Thiel, W. *J. Am. Chem. Soc.* **1977**, *99*, 4899, 4907. (b) Stewart, J. J. P. *QCPE Bull.* **1985**, *5*, 62; *MOSOL Manual*; USAF: Colorado Springs, CO, 1984. (c) Lee, Y. S.; Kertesz, M. *J. Chem. Phys.* **1988**, *88*, 2609.

(12) Dewar, M. J. S.; Yamaguchi, Y.; Suck, S. H. *Chem. Phys.* **1979**, *43*, 145.

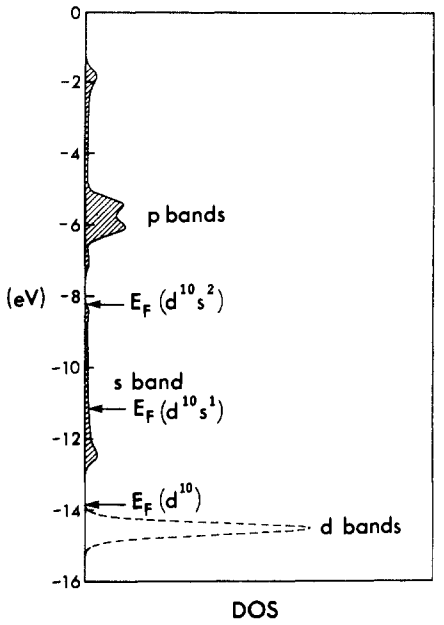

Figure 1. EHT density of states for a linear silver chain. (E_F is the Fermi level; the Ag–Ag separation is 3.03 Å.)

The EHT parameters used are listed in the Appendix. The calculations are based on the energy band theory formalism, which is the **k**-space variant of molecular orbital theory and which properly takes into account a screw axis of symmetry of solids[13] or the translational symmetry, whichever the case may be. Isolated single chain as well as full three-dimensional calculations have been done on the various models referred to in this paper. We also use crystal orbital overlap population (COOP) curves,[13c] which are essentially energy-dependent differential overlap population curves and which are helpful to elucidate the different atomic orbital contributions to the bonding in extended systems.

Bonding in a Silver Cation Chain and Related Compounds

A Linear Ag^+ Chain. Let us begin with the zigzag silver cation chain in $Ag_3(NSO_2)_3$. Here $(NSO_2)_3$ forms a six-membered ring with an alternating arrangement of N and S atoms and receives formally three electrons from three Ag atoms (see **2**). Figure 1 shows the density of states (DOS) for a linear silver chain with an observed bond length of 3.03 Å. The DOS for the planar zigzag silver cation chain is quite similar to that of the linear chain. Figure 1 reveals that due to the interactions between silver atoms, the 5s and 5p energy levels form broad bands and the 4d levels are only slightly spread because of the contraction of the 4d orbitals. A similar DOS of the linear Ag chain has been calculated by Baetzold.[3c,d] Since Baetzold used a small Ag–Ag distance (2.65 Å), his 4d bands overlap with 5s bands. The gap between the 5s and 4d bands is 1.8 eV and is decreased by 2.7 eV as compared with that for a free silver atom. Thus, the silver cation chain is calculated to be a semiconductor in $Ag_3(NSO_2)_3$. The energy band gap (E_g) as a function of the separation of the silver cations is shown in Figure 2. The band gap as a function of the size of Ag cluster has been discussed by Baetzold, showing a similar trend as shown in Figure 2.[3c,d] A similar curve has been obtained for the zigzag silver cation chain and is not shown here. It can be seen that the band gap is decreased upon reducing the distance between the silver cations. The decrease of E_g primarily comes from the lowering in energy of the 5s and 5p bands as the cations get closer. Therefore, the conductivity of compounds containing silver cations depends largely on the separation of silver cations. This is in agreement with experimental trends in a large number of silver-rich crystals.[8]

The Nature of the Band Gap in Ag_2O. According to the description of silver-rich compounds by Jansen,[8] d^{10} crystals with

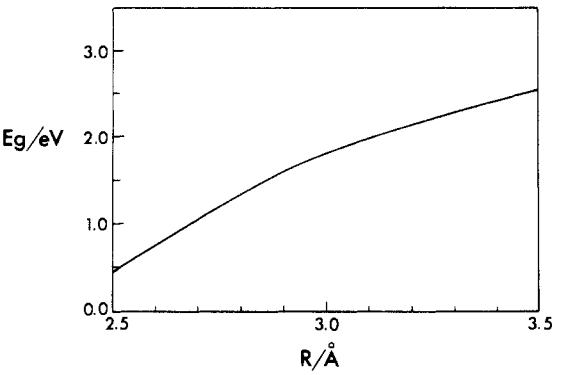

Figure 2. EHT energy band gap (E_g) as a function of metal separation, R, in a linear Ag (d^{10}) cation chain.

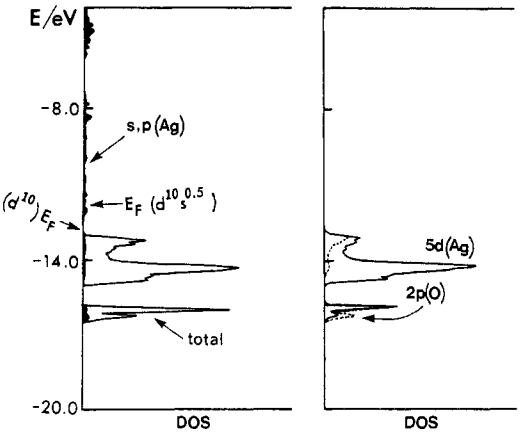

Figure 3. EHT density of states (DOS) and various projected DOS's for Ag_2O. $E_F(d^{10})$ and $E_F(d^{10}s^{0.5})$ correspond to the Fermi levels for Ag_2O and Ag_2F, respectively. For the latter, a rigid band model is assumed.

a silver bond distance comparable to that of metallic silver usually are semiconductors. If the silver–silver separation is large (3.5–4.0 Å), they will be insulators, such as Ag_2SO_4.[14] A typical example of a silver-rich compound is Ag_2O[15] (**6**), which crystallizes in the

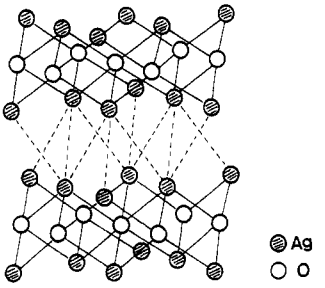

6

anti-CdI_2 structure under pressure and has silver–silver separations of 3.05 Å. Actually, Ag_2O is termed a "layer structure" because it consists of repeat units (or sandwiches) Ag–O–Ag–Ag–O–Ag–Ag–O, where the symbols O and Ag represent layers of those atoms. These layer compounds are interesting in their own right, and we shall see shortly how they will aid us in developing a bonding picture for the chain systems at hand.

The calculated DOS and various projected DOS's based on the observed structure are shown in Figure 3. In agreement with the orbital interaction picture we described above for the linear silver chain, a band gap of 0.54 eV is predicted based on three-dimensional crystal orbital calculations on Ag_2O. The black color

(13) (a) Ashcroft, N. W.; Mermin, N. D. *Solid State Physics*; Saunders: Philadephia, PA, 1976. (b) Kertesz, M. *Adv. Quantum Chem.* **1982**, *15*, 161. (c) Hoffmann, R. *Angew. Chem., Int. Ed. Engl.* **1988**, *26*, 846.

(14) Friebel, C.; Jansen, M. *Z. Naturforsch.* **1984**, *B39*, 739.

(15) (a) Klemet, W., Jr. *Phys. Status Solidi.* **1977**, *A39*, PK45. (b) Werner, A.; Hochheimer, P. *Phys. Rev.* **1982**, *B25*, 5929.

(16) Hoffmann, R. *Angew. Chem., Int. Ed. Engl.* **1987**, *26*, 846.

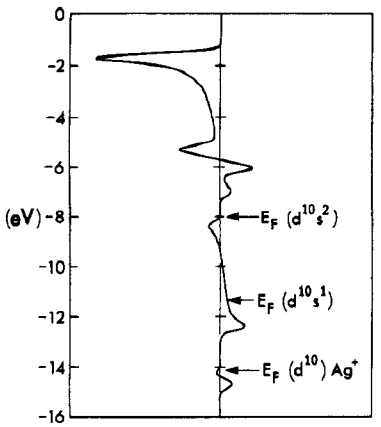

Figure 4. COOP curve for the Ag–Ag bond in a silver chain with a Ag–Ag separation of 3.03 Å, calculated by EHT. (DOS is given in Figure 1.)

of Ag_2O supports the calculated small band gap.[15] This band gap is smaller than that of the linear silver chain because there are nine nearest neighbors for each silver in Ag_2O. In this way, the 5s and 5p bands are lowered even further than in the silver chain. The projected DOS curves show that the conduction bands are mainly 5s and 5p in character and the highest occupied bands are the mixtures of silver 4d and oxygen 2p orbitals. Thus, color and conductivity of silver-rich compounds should come from the electronic transitions between the highest occupied orbitals, which are mixtures of anion p and metal d orbitals, and the levels of the metal aggregates, which are mostly metal s and p in character. Jansen came to a similar conclusion based on chemical intuition and analysis of experimental data for a large number of silver-rich compounds.[8]

Ag–Ag Bonding in Chains and Layers. Let us return to the case of a linear chain and look at the details of metal–metal bonding. Figure 4 shows the COOP curve for Ag–Ag bonds in such a chain. The d-band contributions to the COOP curve, as usual for a simple chain,[13c] are divided into two regions. The first is bonding and comes from the crystal orbitals with energies below −14.6 eV (ionization potential of d orbitals). The second part is antibonding; owing to the mixing of silver 5s and 5p orbitals into 4d orbitals, the bonding contributions are larger than the antibonding ones. As a result, d^{10}–d^{10} repulsions are converted to weakly attractive interaction.[3b] The overlap population between Ag atoms within the Ag^+ chain is 0.04, indicating slight silver–silver bonding. We have obtained the same overlap population (0.04) between silver atoms in adjacent silver layers for Ag_2O. Within the layer the overlap population is 0.024, which is smaller than 0.04. We attribute this to the ligand effect on metal–metal bonding as we will discuss in the following section. This bonding picture is in agreement with that derived by Hoffmann and other authors[3] for some organocopper compounds. Ag_2O provides an excellent evidence that the bare d^{10}–d^{10} interaction is attractive because it lacks bridging ligands holding the Ag^+ ions in adjacent Ag layers together and the Ag–Ag separation is as short as 3.05 Å.

The next part of the COOP curve lying between −12.5 and −9.5 eV is due to silver–silver bonding and corresponds to metal 5s orbitals. If electrons are added to the silver cation chain beyond the d^{10} filling, bonding between silver cations will be strengthened due to the occupation of these silver–silver bonding crystal orbitals. This is indeed the case for the zigzag silver chains in CaAg as indicated by the shorter Ag–Ag distances of 2.88 Å. The calculated overlap populations between silver atoms in CaAg is 0.20. On the basis of Mulliken population analysis obtained from three-dimensional crystal orbital calculations on CaAg, the Ag and Ca atoms are negatively and positively charged by 1.10 e, respectively. Other examples of direct M–M bonding beyond the d^{10} filling include the partially charged mercury cation chains $(Hg^{+1/3})_x$ found in Hg_3NbF_6, in which the shortest and largest separations of mercury cations are 2.59 and 2.98 Å, respectively. The bond-length alternation is induced here by a Peierls distortion,[17] as pointed out previously,[18] because of the presence of a

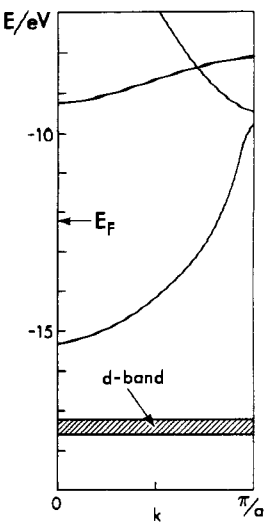

Figure 5. EHT band structure of a linear Hg chain. (The Hg–Hg separation, a, is 2.90 Å; E_F is the Fermi level corresponding to $Hg^{+1/3}$.)

partially filled s band, as can be seen from the band structure of linear Hg atom chain in Figure 5.

Another interesting example is Ag_2F,[19] which is structurally similar to Ag_2O, where the Ag atom is not d^{10} but $d^{10}s^{0.5}$. The overlap population between silver atoms in adjacent layers is calculated to be 0.11 in Ag_2F, showing some bonding. According to the experimental result, Ag_2F is metallic and its conductivity is high. On the basis of the rigid band model, Ag_2F has a partially filled band as indicated by Figure 3.

Considering such a chain, an interesting issue is whether the linear or the zigzag conformation is energetically more favorable. The calculated energy difference, however, is small. For bond angles of 120 and 180° and a uniform Ag–Ag separation of 3.03 Å, the zigzag chain is calculated to be slightly more stable than the linear one by about 0.3 kcal/mol. This is because the mixing of 5s and 5p orbitals into 4d orbitals on silver can be maximized in the zigzag conformation.

Let us return now to the bridged chains. As it turns out, the ligands play a predominant role in determining M–M bonding in these structures.

M–M Bonding in the A_nMR Types

As we have pointed out in the introduction, metal–metal bonding in the d^{10} chains collected in Tables I and III should be quite weak and is expected to be very different from that in CaAg and Hg_3NbF_6 where metal–metal bonding is significant. The following analysis of metal–metal bonding in two typical chains, Na_2CuP and HgO, will demonstrate this point.

Metal-Metal Bonding in Na_2CuP with a Bridged Ligand. Since the one-dimensional chains listed in Table I have a 2-fold screw axis of symmetry, we will use this symmetry in this section in order to simplify solid-state calculations and facilitate the interpretation of the band structure. Let us begin with a simple discussion on helical symmetry. Each irreducible representation of the Abelian group formed by operators of a screw axis of symmetry can be indexed by a vector. These vectors correspond one by one to the wave vectors in the Brillouin zone (BZ) defined by the basic translation vector **h** in direct space, which has the same length as the translation part of the screw operation. The vectors in the BZ can be used for indexing the irreducible representation of the above Abelian group.[7,13] However, the symmetry-adapted linear combination of atomic orbitals for polymers under the operation of a screw axis of symmetry has a different nodal structure from that under the operation of a simple translation symmetry even when both have the same wave vector. Therefore, the BZ used

(17) Peierls, R. E. *Quantum Theory of Solids*; Oxford University Press: London, 1955.
(18) Kertesz, M.; Guloy, A. M. *Inorg. Chem.* **1987**, *26*, 2852.
(19) Argay, G.; Naray-Szabo, F. *Acta Chim. Acad. Sci. Hung.* **1966**, 329.

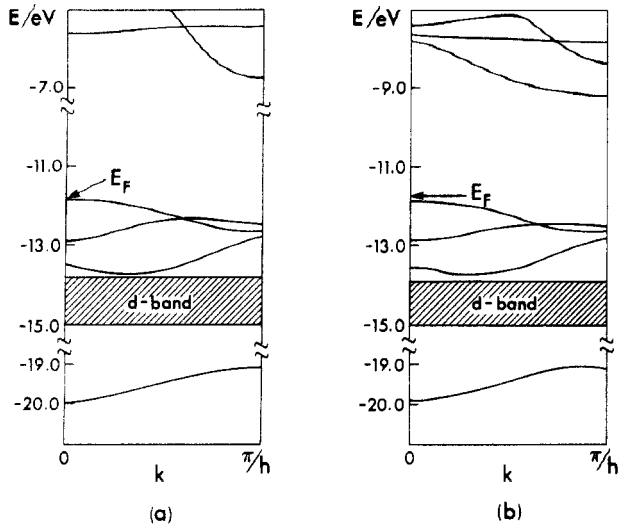

Figure 6. EHT band structures for a zigzag $(CuP^{2-})_x$ chain without (a) and with (b) 3d orbitals on P.

Table IV. Calculated Band Gaps (eV) of Selected Polymers (EHT)

polymer	E_g(sp)[a]	E_g(spd)[a]	polymer	E_g(sp)[a]	E_g(spd)[a]
Na_2CuP	4.97	2.75	KAuSe	7.46	2.65
KCuS	5.84	2.52	AuCl	7.86	3.90
KAuS	6.61	2.99	AgCNO	3.77	

[a] sp and spd bases are used and are given in Table VII.

for the helical group is called the pseudo-Brillouin zone (PBZ).[20] The band structure in this section will be represented in the PBZ.

Because of the low 4s ionization potential of Na and the quite weak covalent bonding between Cu and Na atoms as well as between P and Na atoms, complete charge transfer from Na to the chains may be assumed and the zigzag $(CuP^{2-})_x$ chains in Na_2CuP can be considered to be well separated. The band structure of this chain is shown in Figure 6a in the absence of 3d orbitals on P, indicating an indirect band gap of 5.01 eV. The $(CuP^{2-})_x$ chain is predicted to be an insulator at this level of approximation. If the 3d orbitals on P are taken into account in the calculation, this essentially does not change the occupied bands as shown in Figure 6b. The Fermi level E_F is only decreased from 11.85 to 11.92 eV. However, the unoccupied bands are significantly pushed down in energy, especially the first conduction band. Similar situations have been found in elemental silicon and selenium where d orbitals play a very important role in the semiconducting properties.[21,22] The calculated band gap for Na_2CuP is 2.75 eV, including 3d orbitals on P atom. Therefore, we expect Na_2CuP to be a large gap semiconductor or an insulator. This conclusion holds for the crystals listed in Table I with anions as ligand. Calculated band gaps for some selected compounds are listed in Table IV.

The calculated charge distribution for the $(CuP^{2-})_x$ zigzag chain indicates that Cu is charged by −0.17 and P by −1.83 as estimated by gross atomic Mulliken population. On the basis of the experience of the previous analysis of Ag–Ag bonding in the silver chain, one might expect that there should be some Cu–Cu bonding in this chain because the electronic configuration of Cu in the $(CuP^{2-})_x$ zigzag chain is not d^{10} but $d^{9.89}s^{0.81}p^{0.47}$, similar to that of Ag ($d^{9.94}s^{1.42}p^{0.74}$) in CaAg. In fact, the calculated Cu–Cu overlap population is 0.03, which is much smaller than the silver–silver overlap population of 0.20 in CaAg. Moreover, it is even smaller than the value of 0.07 between copper d^{10} centers for a bare Cu^+ chain with the same Cu–Cu distance as in $(CuP^{2-})_x$. With the inclusion of 3d orbitals on the ligands, the Cu–Cu overlap population comes out to be 0.02, a value only slightly smaller than

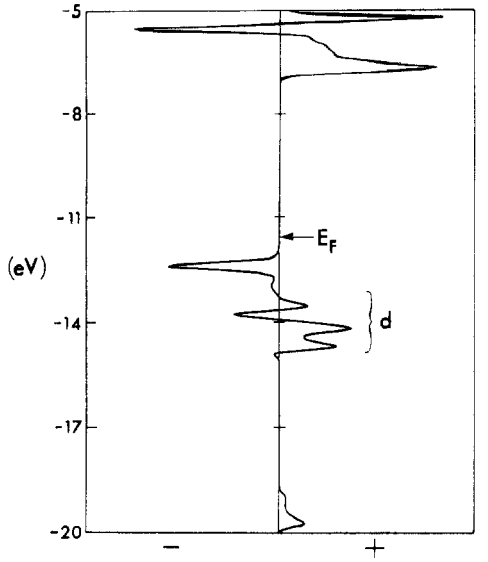

Figure 7. COOP curve for the Cu–Cu bond in the $(CuP^{2-})_x$ zigzag chain by the EHT method. Total overlap population is 0.03 with the corresponding Fermi level indicated by E_F.

that without 3d orbitals. Therefore, there is a significant effect of ligand d orbitals on Cu–Cu bonding.

Let us turn to the Cu–Cu COOP curve of $(CuP^{2-})_x$ zigzag chain, as shown in Figure 7, which will help us to figure out the story behind this small overlap population. The COOP curve for Cu–Cu bond in the range between −20.0 and −18.0 eV has a bonding contribution. The corresponding representative orbital interaction picture is illustrated by **7** at $\mathbf{k} = 0$. The crystal orbitals

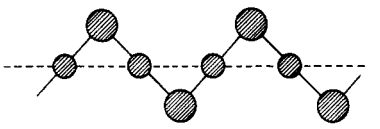

7

lying in this energy region have mainly P (3s) and Cu (4s) character. These 4s orbitals form bonding combinations between metal centers. The crystal orbitals lying in energy between −13.0 and −12.0 eV are metal-metal antibonding and are schematically shown in **8** at $\mathbf{k} = \pi/h$. They are antibonding between the 4s

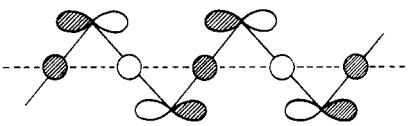

8

orbitals on metal atoms and bonding between the metal and ligand orbitals. As a result of the bonding interaction of metals and ligands, the above energy region is somewhat lower than the value of the Cu (4s) ionization potential. Thus, the metal–metal bonding contributions from **7** are largely compensated for by the occupation of the metal–metal antibonding crystal orbitals **8**. At the same time, the bonding contributions to metal–metal bonding from the mixing of 4s, 4p, and 3d orbitals on Cu, a mixing earlier identified as being responsible for d^{10}–d^{10} bonding in Cu complexes[3], are partially cancelled because of the occupation of metal–metal antibonding crystal orbitals like **8**. This explains why the overlap population between metal centers in the $(CuP^{2-})_x$ chain is smaller than that between pure d^{10} centers in the absence of ligands. The net result is that the metal 4s and 4p orbitals are used for metal–ligand bonding rather than for metal–metal bonding. This differs from the CaAg case where valence s and p orbitals on silver are used for silver–silver bonding. The short Cu–Cu separation comes from the requirement of the favorable metal–ligand bonding, that is, from through-light coupling, which is quite similar

(20) (a) Blumen, A.; Merkel, C. *Phys. Status Solidi* **1977**, *B83*, 425. (b) Karpfen, A. *J. Comput. Chem.* **1984**, *5*, 11.
(21) Biswas, R.; Kertesz, M. *Phys. Rev.* **1984**, *B29*, 1791.
(22) Cui, C. X.; Jiang, Y. *Wuli Huaxue Xuebao* **1987**, *3*, 581.

to through-bond interactions.[23] Therefore, despite large overlap integrals between copper atomic orbitals, only slight bonding occurs.

A similar decrease of Cu–Cu bonding upon inclusion of ligands has been found in $[Cu(tolylNNNNNtolyl)]_3$[3a,24] where the Cu–Cu bond distance of 2.35 Å is the shortest one that has been recorded up to now. The Cu–Cu overlap populations for this complex with or without ligands are 0.127 and 0.132,[3a] respectively. This slight decrease is also due to the occupation of Cu–Cu antibonding molecular orbital, which is derived from a valence molecular orbital of the linear Cu_3 cluster as shown in **9**.

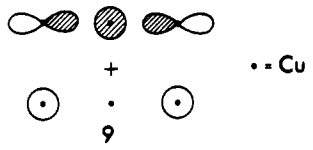

9

The Case of HgO—No d^{10}–d^{10} Bonding in a Bridged Chain. A completely different situation arises for the systems in Table III, HgO being a typical example (**4**) with a large metal–metal separation of 3.28 Å. Let us defer the issue of planarity vs helical configuration of these chains to the next section and focus on metal–metal bonding. Therefore, a planar model of HgO will be considered here. The calculated overlap population between Hg atoms of the experimental zigzag HgO chain is −0.02. This indicates that there is no bonding between Hg atoms in HgO. We have performed a model calculation for the $(CuP^{2-})_x$ chain where Cu–P distance is kept at the experimental value of 2.24 Å and the Cu–Cu separation is increased to 3.30 Å. The resulting Cu–Cu overlap population decreased from +0.024 to −0.005. These negative overlap populations result from the occupation of the crystal orbitals that are slightly metal–metal antibonding (**8**). The orbital interaction scheme and the COOP curve for Hg–Hg bonding in HgO are basically similar to those for Cu–Cu bonding in Na_2CuP. Figure 8 shows the COOP curve for a Hg–Hg bond in a planar model of the HgO chain. The antibonding contributions to Hg–Hg bonding below the Fermi level are larger than the bonding ones, and the reverse is true for Figure 7. Still the two cases are very similar in that the positive and negative contributions almost cancel. The above analysis also offers an explanation of the negative overlap population between Cu centers in $Cu_8S_{12}^{4-}$.[3d]

Role of Ligands. There are three different kinds of ligands in the compounds listed in Table I.

The first kind are typical two-electron donors like CNO^- and CR_3^- found in other organocopper compounds[25,3b] as, e.g., in **10**.

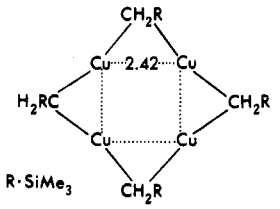

10

The polymers having this kind of ligand usually have metal–metal separations comparable to that of the corresponding elemental metals and acute M–L–M bond angle because of the formation of the three-center two-electron bonds as shown in **11** where the

11

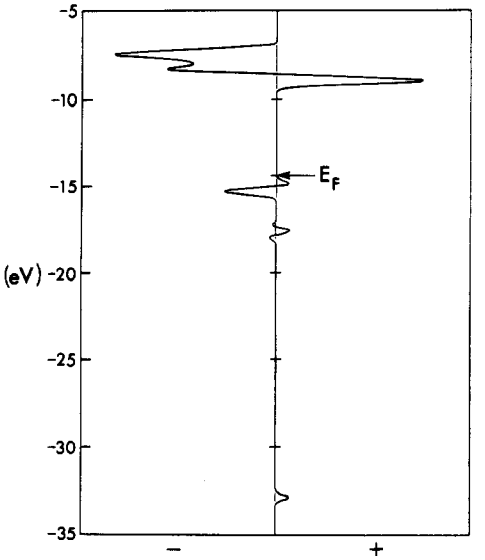

Figure 8. COOP curve for the Hg–Hg bond in the HgO polymer. Total overlap population is −0.02.

metal is in an sp state.[25b] For this situation, some metal–metal bonding is expected. Indeed, the calculated Ag–Ag overlap population of AgCNO chain is 0.07.

The second type is a typical four-electron donor such as NH_2^- and NCO^-. The polymers with such ligands are more likely to have the M–L–M angle larger than 90° and large metal–metal separations. It is easy to understand the underlying electronic factors if one realizes that there exist two-center–two-electron bonds between two metal atoms and the bridging ligand. This is illustrated in **12** for the case of a ligand atom in sp^3 hybridization. The sp^2 case is similar and is not shown here.

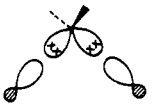

12

The third kind of ligands is anions of main group atoms. It is difficult to say whether these ligands are two-electron or four-electron donors. However, formally one could consider these atoms to be in a state of sp^3 hybridization. Then, they could become either two-electron donors to adopt the three-center–two-electron bonds like **11** or four-electron donors to adopt the two-center–two-electron bond scheme as illustrated in **12**. At the present level of theory, it is hard to tell which situation is energetically more favorable. Examination of the ligands indicates that if the ligand is an anion and has large polarizability, the polymer is more likely to be closer to the bonding scheme **11** and if the ligand is less polarizable, the chain prefers the bonding type **12**. This is illustrated best by the example of the auric halides: from AuCl[10] to AuI the MLM angle decreases from 92 to 72°, and for AuBr there are two crystalline modifications: one with 92° and another one with 77°. Obviously, if there is any Au–Au bonding in the one with the smaller MLM angle, it has to be rather weak, as supported by the bonding scheme outlined above and the corresponding small M–M overlap populations.

Metal–Metal Bonding in a Chain without Bridged Ligands. The ligands we discussed above (P^{3-}, O^{2-}) essentially do not induce any metal–metal bonding. But the ligands in $[Ag(CCR)_2Ag(PPh_3)_2]_x$[26] (**13**) and $[AuI(S(CH_2)_4]_x$, where metal atoms have a formal electronic configuration of d^{10}, strengthen a pure d^{10} interaction. $[AuS(CH_2)_4I]_x$ has a structure similar to that of **13** and is not shown here. For **13**, the separation of silver atoms is 3.03 Å, and Ag has a formal electronic configuration of d^{10} when considering that the Ag atom coordinated by CCR gives two

(23) Hoffmann, R. *Acc. Chem. Res.* **1971**, *4*, 1.
(24) Beck, J.; Strahle, J. *Angew. Chem., Int. Ed. Engl.* **1985**, *24*, 409.
(25) (a) Jarvis, J. A.; Kilbourn, B. T.; Pearce, R.; Lappert, M. F. *J. Chem. Soc., Chem. Commun.* **1973**, 475. (b) Wardell, J. L. In *Comprehensive Organometallic Chemistry*; Wilkinson, G., Ed.; Pregamon Press: New York, 1982; Vol. 2.
(26) Corfield, P. W. R.; Shearer, H. M. M. *Acta Crystallogr.* **1966**, *20*, 502.

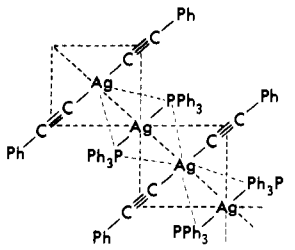

13

electrons to two CCR groups and receives one electron from the Ag atom coordinated by PPh_3. The calculated charges on the Ag atoms coordinated by CCR and PPh_3 are −0.01 and −0.09 e, respectively. The calculated overlap population is 0.07 between Ag atoms, which is larger than 0.04 for the naked d^{10} centers, as in Ag_2O. For these two one-dimensional chains, there is unquestionably some metal–metal bonding, but the bonding still is quite weak.

What is the difference between the bridging and nonbridging ligands in influencing metal-metal bonding? Let us see what happens if we increase the Cu–Cu–ligand bond angle from the experimental value of 51.7° to 90° for $(CuP^{2-})_x$, i.e. move all the ligands parallel to the chain from a bridging to a nonbridging position. Obviously, orbital **8** no longer exists because the symmetry of the 3p orbital on P in **8** is different from that of the 4s orbital on Cu. Two orbitals can be derived from **8**. The first is the lone-pair 3p orbital on P which is occupied. The second is the metal–metal antibonding orbital, which is empty. Therefore, some additional metal–metal bonding is expected relative to the bridged situation. Indeed, the calculated overlap populations listed in Table V illustrate this effect. However, it can not be said that every bridging ligand would reduce metal–metal bonding. Only bridging ligands, which could produce orbitals like **8**, would weaken metal–metal bonding. This is illustrated best by **10**, in which CR_3^- is a typical two-electron σ donor, where the orbitals like **8** are absent due to symmetry reasons. Here, some metal–metal bonding should be induced by the ligand. We have performed EHT calculations on the hypothetical chain $(CuCH_3)_x$ where the Cu–Cu, Cu–C, and C–H separations are 2.44, 2.00, and 1.10 Å, respectively, and the structure is the same as in $(CuP^{2-})_x$. The calculated Cu–Cu overlap populations without and with the inclusion of CH_3^- ligands are 0.10 and 0.14, respectively, proving the different roles played by such ligands, as opposed to P^{3-}, in influencing d^{10}–d^{10} bonding.

Helical Polymers

Binary mercury compounds to main-group group 6 atoms usually exist in the zinc blende structure[2] or a hexagonal form that is built of helical chains. Mercuric oxide and sulfide are found in a helical conformation under normal conditions. But hexagonal mercuric selenide and telluride exist only under high pressures. What the driving force to make them assume a helix is has not been investigated theoretically up to now, although the electronic reasons responsible for the screw configuration of some main-group polymers have been elucidated recently.[7]

Before starting to discuss the mercuric oxide helix, it is useful to review the factors responsible for the helical structure of polymeric sulfur.[7] Zigzag polymeric sulfur has a completely filled broad π band that produces a repulsion similar to the so-called four-electron repulsion in molecules.[27] The loss of energy due to electron repulsion has an approximately quadratic relationship with the band width.[7] The effect of the completely filled π band of polymeric sulfur on its geometry is to drive it toward a screw configuration.[7]

Fortunately, MNDO parameters for mercury (no d orbitals included) are available.[28] This makes it possible to obtain potential energy surfaces of mercury oxide and sulfide helical chains at that level of theory. Figure 9 shows the torsional potential curves of these two polymers. Only one minimum for each polymer has been located on the corresponding MNDO energy surface of the isolated chains. The optimized structure corresponds to the planar zigzag conformation. Although no other minima have been found on the energy surfaces for helical HgO and HgS, the torsional potential curves are very flat between helical angles of 180 and 120°. The calculated heat of formation per HgO or HgS repeat unit is increased by a mere 0.2 kcal/mol upon the decrease of the helical angle from 180° (linear zigzag) to 120° (experimental 3-fold helix). Therefore, due to the favorable crystal packing effects, HgO and HgS chains can exist in helical structures.

The orbital interaction illustrations for the energy surfaces of HgO and HgS are presented in **14**. Formally, HgS can be

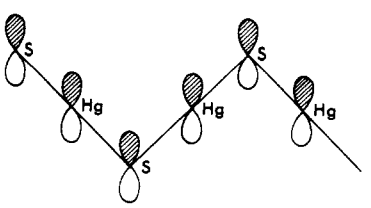

14

considered to be formed by inserting a Hg atom into the middle of every S–S bond of a zigzag polymeric sulfur chain. Because of the empty p_z orbital on Hg, the interaction between this orbital and the sulfur p_z lone-pair orbital converts the lone-pair repulsions to π bonding. Any distortion from the planar zigzag structure will lead to a decrease of this weak π bonding between mercury

Table V. Overlap Populations for Different Metal–Metal–Ligand Bond Angle for Several Selected Chains

chain	MML bond angle, deg	overlap popn
$(CuP^{2-})_x$	53.9[a]	0.026
	90.0[b]	0.068
$(AgAs^{2-})_x$	56.3[a]	0.036
	90.0[b]	0.071

[a] Experimental value, bridged chain. [b] Ligands in nonbridging position.

Table VI. MNDO Optimized Geometrical Parameters for HgO and HgS

	bond length, Å		bond angles, deg		dihedral angles, deg	
polymer	Hg–X	Hg–Hg	HgXHg	XHgX	XHgXHg	HgXHgX
HgO	1.95	3.40	121.6	179.4	180.0	180.0
HgO (helix)[a]	1.94	3.38	120.0	177.1	53.6	163.9
HgS	2.22	3.37	99.0	179.4	180.0	180.0
HgS (helix)[a]	2.21	3.34	102.7	170.4	107.5	143.2

[a] Corresponding fixed helical angle of 120.0°.

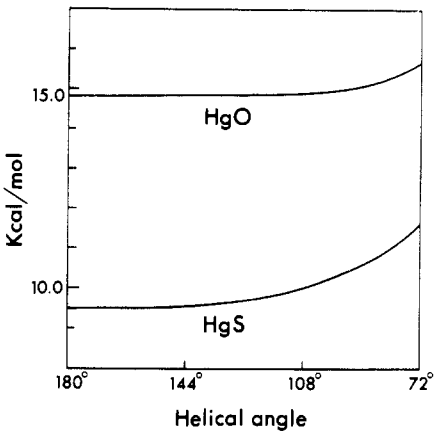

Figure 9. MNDO torsional potential curve (heat of formation per repeating unit as a function of helical angle as depicted in **5**) for HgO and HgS helical chains.

(27) For a review see: Albright, T. A.; Burdett, J. K.; Whangbo, M.-H. *Orbital Interaction in Chemistry*; John Wiley & Sons: New York, 1985.
(28) Dewar, M. J. S.; Grady, G. L.; Merz, K. M., Jr.; Stewart, J. J. P. *Organometallics* **1985**, *4*, 1964.

Table VII. EHT Parameters Used

atom	orbital	H_{ii}, eV	ζ_1	C_1	ζ_2	C_2
Hg	6s	−13.68	2.649			
	6p	−8.47	2.631			
	5d	−17.50	6.436	0.6438	3.032	0.5215
Cu	4s	−11.40	2.200			
	4p	−6.06	2.200			
	3d	−14.00	5.950	0.5933	2.300	0.5744
Ag	5s	−11.16	2.240			
	5p	−5.81	2.200			
	4d	−14.54	6.070	0.5889	2.663	0.6370
Ca	4s	−7.00	1.200			
	4p	−4.00	1.200			
P	3s	−18.60	1.880			
	3p	−12.50	1.630			
	3d[a]	−7.00	1.400			
S	3s	−20.00	2.120			
	3p	−13.30	1.830			
	3d[a]	−8.00	1.500			
Cl	3s	−30.00	2.360			
	3p	−15.00	2.040			
	3d[a]	−9.00	2.033			
Se	4s	−20.50	2.430			
	4p	−14.40	2.070			
	4d[a]	−8.00	0.900			

[a] Optional d orbitals have been included as indicated in text.

and the oxygen or sulfur p_z orbitals.

Table VI lists the optimized geometrical parameters for HgO and HgS for two conformations. The first one is the zigzag conformation and the second is the helical configuration with a experimental helical angle of 120°. In comparison with experimental structures, the Hg–X (X = O, S) bond length is shorter by about 0.1 Å, and the Hg–X–Hg bond angle for HgO is larger by about 12° and for HgS is smaller by about 2°.

For the MNDO-optimized geometries, the calculated extended Hückel band gaps for the planar zigzag form of HgO and HgS are 5.35 and 4.02 eV and for the helical form are 5.85 and 4.58 eV, respectively, indicating that they are insulators.[5]

Conclusion

In summary, d^{10}–d^{10} bonding in crystals containing one-dimensional bridged or unbridged chains of metal atoms is analyzed by performing extended Hückel calculations on various model chains as well as related three-dimensional structures. For the chains, the experimental observations show the following trends. First, metal–metal (Cu–Cu, Ag–Ag, Au–Au, Cd–Cd, and Hg–Hg) bond distances in d^{10} metal chains exhibit a large variety, the closest contacts being even shorter than in the elemental metals. Second, the metal–metal distances play an essential role in determining the color and conductivity of related silver-rich compounds. We give theoretical evidence for covalent directional bonding between the metals and the ligands, which are responsible for the large variety of metal–metal bond distances. Color and conductivity of the silver-rich compounds are primarily determined by the distance of d^{10} centers or d^{10}–d^{10} interactions.

The calculations show that, from the point of view of metal–metal bonding, the compounds fall into two main categories. In the first group, in which an anion of a main-group atom is the bridging ligand, there is slight or no M–M bonding due to the effect of the ligand which reduces the metal–metal bonding between naked d^{10} centers. The short M–M bond distances for some of these chains comes from metal–metal coupling through the ligands. A typical example of such a compound is Na_2CuP. In the second group in which bridging ligands are absent, such as $[Ag(CCR)_2(PPh_3)]_x$, there is some M–M bonding, producing the short M–M bond distances.

The analysis of orbital interactions shows that if the bridging ligand is a typical two-electron σ donor, such as CH_3^-, direct metal–metal bonding is induced by the ligand.

Our calculations on the silver-rich Ag_2O phase indicate that the color and conductivity for a number of silver-rich compounds result from excitation from oxygen 2p and metal 4d orbitals to metal 5s and 5p orbitals. Decrease of the Ag–Ag distance will lead to decrease of the gap between 4d and 5s bands, which in turn gives rise to various colors and conductivities.

Our calculations show that the helical conformation of mercuric sulfide and oxide can be attributed to the crystal packing since the calculated torsional potential curves are very flat over a broad range of twist angles.

Appendix

The parameters[3,18,29] used in this work are listed in Table VII. In the calculations of average properties, **k**-point sets with 50 and over 190 **k** points have been used for one- and three-dimensional crystals, respectively.[30] The N, O, and C parameters used are standard values. Unless noted otherwise, the structures used for the calculations are based on experimental data.

Acknowledgment. This work was supported by the National Science Foundation through Grant DMR-8702148 and the Camille and Henry Dreyfus Foundation (1984–1989). We are indebted to Ann Pope for the skillful drawings.

(29) (a) Burdett, J. K. *Molecular Shapes*; John Wiley & Sons: New York, 1980. (b) Whangbo, M. H. *Solid State Commun.* **1982**, *43*, 637. (c) Zheng, C.; Hoffmann, R.; Nesper, R.; Von Schnering, H. G. *J. Am. Chem. Soc.* **1986**, *108*, 1876.

(30) Pack, J. D.; Monkhorst, H. J. *Phys. Rev.* **1977**, *B16*, 1748.